On some integration schemes for rate equations of damaged elastoplastic solids

Karim Nesnas* — Fafa Benhatira* — Smail Bezzina* — Khemais Saanouni**

** LG2ms/Mécanique URA1505 du CNRS*
Université de Technologie de Compiègne, B.P 529, 60205 Compiègne cedex

*** GSM/LASMIS*
Université de Technologie de Troyes, BP 2058, 10010 Troyes cedex

ABSTRACT. *This work is concerned with the study of some numerical procedures used for the integration of damaged elastoplastic constitutive equations which exhibit some induced softening (or negative hardening) due to the damage effect. For this purpose, various integration procedures are used. The implicit schemes are represented by the radial-return and the generalized trapezoidal (or mid-point) algorithms modified to enhance the consistency condition during the softening stage. The explicit schemes are represented by only the fourth order Runge-Kutta algorithm in connection with two different techniques of automatic time step size control. The efficiency and robustness of the studied solution procedures are evaluated with numerical tests using both the single Gauss point and the cantilever beam structure.*

RÉSUMÉ. *Ce travail est consacré à l'étude des performances des schémas d'intégration numérique des équations de comportement de solides élastoplastiques endommageables ayant la particularité d'avoir un écrouissage négatif qui succède à l'écrouissage positif. Pour ce faire, une variété de méthode d'intégration a été utilisée. Les algorithmes implicites sont représentés par la méthode du retour radial généralisée et la méthode du trapèze généralisée modifiée pour satisfaire la condition de consistance par une correction de contrainte basée sur l'algorithme précédent. Les algorithmes explicites sont représentés par le seul schéma de Runge-Kutta d'ordre 4 mais avec deux techniques différentes de calcul automatique de la taille du pas. L'efficacité et la robustesse de ces méthodes sont évaluées sur des tests numériques au niveau d'une structure simple.*

KEY WORDS : *finite elements, implicit algorithm, Runge-Kutta, stepsize control, damage, plasticity.*
MOTS-CLÉS : *éléments finis, algorithme implicite, Runge-Kutta, contrôle du pas, endommagement, plasticité.*

Revue européenne des éléments finis. Volume 5 - n° 4/1996, pages 491 à 519

1.Introduction

Since the great development of the numerical methods for mechanical engineering analysis, many studies have been published concerning the numerical integration of various constitutive equations as a highly non-linear differential partial equations (see the recent book by Crisfield [CRI 91] and the references given there). For the particular case of the elastoplastic and elasto-viscoplatic constitutive equations developed in the framework of the thermodynamics of irreversible processes with state variables [LEM 85], many works concerned with numerical integration schemes of the associated constitutive equations have been published ([NGU 72], [GEL 85], [ORT 86], [SIM 87], and [GOL 89],..). Recently, in [TOU 93] the numerical aspects of the integration of elastoplastic constitutive equations without damage have been studied, i.e., having only a positive strain hardening. After comparing some integration schemes, they show that the Runge-Kutta algorithm with automatic step size controls is particularly efficient compared to the generalised Trapezoidal algorithms.

Therefore the numerical integration of the constitutive equations coupled with the continuous damage mechanics have been much less studied in the literature ([CHA 77, 78], [SIM 86], [BEN 89], [GEL 92] , [SAA 94], [FOR 95],...). In fact for this type of coupled constitutive equations, characterised by the damage induced softening, a special care must be taken to enhance the efficiency of the used integration scheme in the post-critical stage (i.e. softening stage).

The present work is an extension of the work presented in [TOU 93] to the coupled elastoplastic constitutive equations with damage softening effect. Both the explicit and implicit integration scheme are studied. The fourth order Runge Kutta Algorithm (RKA - RKB) associated to two different techniques of automatic step size control as an explicit scheme, while the implicit scheme are represented by the Return Mapping Algorithm (RMA) as well as the generalised Trapezoidal Algorithm (GTA). The accuracy, the numerical stability, the CPU time and the enforcement of the consistency condition of each used algorithm are studied and compared using some numerical tests at Gauss point and using a simplified structure used by [TOU 93]. In section 2, the coupled constitutive equations proposed in [SAA 93] are recalled and written under a suitable form. The section 3 is devoted to the presentation of the studied integration schemes while the section 4 is concerned with the application to both the simple Gauss point (material point) and a simple structure (bending beam).

2 Equations of elastoplastic flow with damage:

In this section, the formulation of the basic equations of the constitutive model is considered, based on the thermodynamics of irreversible processes with internal variables. This damage-elastoplasticity model adopts the following hypothesis: i)

small displacements and strains , ii) linear, isothermal and isotropic elastic behaviour, iii) isotropic plastic flow of Mises type with non-linear isotropic and kinematic hardening. iv) isotropic plastic (ductile) damage. All these phenomena are represented by the following couples of state variables :

* The observable State Variables (OSV)

$(\varepsilon_{ij}, \sigma_{ij})$the total strain tensor and the associated Cauchy stress tensor.

* The Internal State Variables (ISV)

$(\varepsilon^e_{ij}, \sigma_{ij})$ the elastic strain tensor and the associated Cauchy stress tensor representing the elastic behaviour.

(α_{ij}, X_{ij}) the Kinematic internal strain tensor and the associated internal stress tensor representing the kinematic hardening.

(r, R) the isotropic internal strain tensor and its associated internal stress representing the isotropic hardening.

(D, Y) the isotropic damage and its associated internal force representing the isotropic damage.

Since the effect of the damage in the elastoplastic behaviour can not be neglected, the hypothesis of total energy equivalence is used to define the following so-called effective state variables $(\tilde{\sigma}_{ij}, \tilde{\varepsilon}^e_{ij}), (\tilde{X}_{ij}, \tilde{\alpha}_{ij})$ and $(\tilde{R}, \tilde{r})$. These effective state variables are used in the state and dissipation potentials to derive the constitutive equations fully coupled with damage. The explicit form of thus potentials as well as the detailed calculations to derive the fully coupled constitutive equations can be found in [BEN 91]; [SAA 94]; here are only given the final form of the state and the evolution laws:

* *the state laws:*

$$\sigma_{ij} = \left(\frac{\nu E}{(1+\nu)(1-2\nu)}\right)\varepsilon^e_{kk}\delta_{ij} + \frac{E}{(1+\nu)}\varepsilon^e_{ij} \tag{2.1}$$

$$X_{ij} = \frac{2}{3}\tilde{C}\alpha_{ij} \tag{2.2}$$

$$R = \tilde{Q}r \tag{2.3}$$

$$Y = Y_\sigma + Y_X + Y_R \tag{2.4.a}$$

with

$$Y_\sigma = \frac{1}{2}\frac{J_2^2(\sigma_{ij})}{E(1-D)^2}\sigma^* \tag{2.4.b}$$

$$Y_X = \frac{1}{2\tilde{C}} J_2^2(X_{ij}) \tag{2.4.c}$$

$$Y_R = \frac{1}{2\tilde{Q}} R^2 \tag{2.4.d}$$

with the following notations being used:

$$\tilde{E} = (1-D)E, \quad \tilde{C} = (1-D)C, \quad \tilde{Q} = (1-D)Q$$

and $$\sigma^* = \frac{2}{3}(1+\nu) + 3(1-2\nu)\left(\frac{\sigma_H}{J_2(\sigma_{ij})}\right)^2$$

where, C and Q are the kinematic and isotropic hardening moduli, σ_H is the hydrostatic stress, E and ν are the classical elastic properties of the isotropic medium and $J_2^2(Z_{ij})$represents the Von-Mises norm defined in the stress space by:

$$J_2^2(Z_{ij}) = \frac{3}{2} Z_{ij}^d Z_{ij}^d \tag{2.5}$$

where, $Z_{ij}^d = Z_{ij} - \frac{1}{3} Z_{kk}\delta_{ij}$ is the deviatoric part of the stress tensor Z_{ij}..

* *the evolution laws:*

if $(s_{ij} - X_{ij})\dot{\varepsilon}_{kl} \leq 0 \Rightarrow$ elastic unloading

$$\dot{\sigma}_{ij} = L^{\sigma_e}_{ijkl}\,\dot{\varepsilon}_{kl} \tag{2.6}$$

with $L^{\sigma_p}_{ijkl} = L^{\alpha}_{ijkl} = L^{r}_{ij} = L^{D}_{ij} = 0$

if $(s_{ij} - X_{ij})\dot{\varepsilon}_{kl} > 0 \Rightarrow$ damage-plastic loading

$$\dot{\varepsilon}_{ij} = \dot{\varepsilon}^e{}_{ij} + \dot{\varepsilon}^p{}_{ij} \tag{2.7}$$

$$\dot{\sigma}_{ij} = L^{\sigma}_{ijkl}\dot{\varepsilon}_{kl} \tag{2.8}$$

$$\dot{\alpha}_{ij} = L^{\alpha}_{ijkl}\dot{\varepsilon}_{kl} \tag{2.9}$$

$$\dot{r} = L^{r}_{ij}\dot{\varepsilon}_{ij} \tag{2.10}$$

$$\dot{D} = L^{D}_{ij}\dot{\varepsilon}_{ij} \tag{2.11}$$

where the final forms of the operators L^{σ}_{ijkl}, L^{α}_{ijkl}, L^{r}_{ij}, L^{D}_{ij} and the tangent elastoplastic module H (strictly positive) are defined as :

* The fourth order operators :

$$L^{\sigma}_{ijkl} = L^{\sigma_e}_{ijkl} + L^{\sigma_p}_{ijkl} \tag{2.12}$$

$$L^{\sigma_e}_{ijkl} = \frac{\nu E}{(1+\nu)(1-2\nu)}\delta_{ij}\delta_{kl} + \frac{E}{(1+\nu)}(\delta_{ik}\delta_{jl} + \delta_{il}\delta_{jk}) \tag{2.12.a}$$

$$L^{\sigma_p}_{ijkl} = -\frac{3}{2}\frac{1}{H}\frac{E}{(1+\nu)J_2}\left[\frac{3}{2}\frac{E}{(1+\nu)J_2}(s_{ij}-X_{ij})(s_{kl}-X_{kl}) + \frac{Y^*}{\sqrt{1-D}}(\sigma_{ij}-X_{ij})\sigma_{kl}\right] \tag{2.12.b}$$

$$L^{\alpha}_{ijkl} = \frac{9}{4}\frac{1}{H}\frac{E}{(1+\nu)J_2}\left[\frac{(s_{ij}-X_{ij})(s_{kl}-X_{kl})}{J_2} - \frac{a}{C}\frac{(s_{ij}-X_{ij})X_{kl}}{\sqrt{1-D}}\right] \tag{2.13}$$

* The second order operators :

$$L^{r}_{ij} = \frac{3}{2}\frac{1}{H}\frac{E}{(1+\nu)}\left[1 - \frac{bR}{Q\sqrt{1-D}}\right]\frac{(s_{ij}-X_{ij})}{J_2} \tag{2.14}$$

$$L^{D}_{ij} = \frac{3}{2}\frac{1}{H}Y^*\sqrt{1-D}\,\frac{E}{(1+\nu)}\frac{(s_{ij}-X_{ij})}{J_2} \tag{2.15}$$

with:

$$Y^* = \frac{1}{(1-D)^{\alpha}}\left[\frac{-Y}{S}\right]^{s} \tag{2.16}$$

and s_{ij} is the deviatoric part of the stress tensor σ_{ij}. and the plastic hardening modulus H given by:

$$H = Q + C + \frac{3}{2}\frac{E}{(1+\nu)} - \left[bR + \frac{3}{2} a \frac{(s_{ij} - X_{ij})X_{kl}}{J_2} \right] + \frac{Y^*}{1-D}\frac{\sigma_y}{2} \qquad (2.17)$$

It is worth noting that the material constants a and b characterise the non-linearity of the plastic hardening and S, s and α characterise the evolution of the ductile damage. So that the equations (2.1) to (2.17) defines completely the fully coupled elastoplastic damaged behaviour under the small strain hypothesis. To generalise these coupled constitutive equations to the large strain case the classical rotated frame formulation is used as can be found in [LAD 80], [DOG 86] or [BEN 94] between many others.

3. Some integration algorithms

The constitutive equations proposed above (first order non-linear differential equations) can be formally written under the following standard form :

$$\dot{\mathbf{y}} = \Phi(\mathbf{y}, t) \qquad (3.1)$$

where the vector **y** represents the set of state variables σ_{ij}, α_{ij}, r, D and $\mathbf{y}$ their time derivatives. These differential equations are highly non-linear particularly when the damage is taken into account. Consequently, a small time step is often required in order to solve these equations without loss of stability.

Note that an acceptable algorithm should satisfy four basic requirements: i) first order accuracy; ii) numerical stability; iii) incremental plastic consistency; iv) low cost. The conditions i) and ii) are needed for reaching convergence of the numerical solution as the time step becomes small, condition iii) is the algorithmic counterpart of the plastic consistency condition.

Various numerical integration algorithms have been used for solving the constitutive equations (2.7-2.11). For all algorithms, the first step is the use of an elastic relationship to update the stresses. If these updated stresses are found to lie within the yield surface, the materiel response at the Gauss point will be assured to have either remained elastic or to have unloaded in an elastic way from the yield surface. In these circumstances there is no need to integrate the constitutive equations. However, if the elastic stresses are outside the yield surface, it is necessary to adopt one of the integration algorithms. All of these latter algorithms, excepting the return mapping algorithm, require the intersection of the elastic stress vector with the yield surface. In such case, the following condition is required to be satisfied :

$$f(\sigma_{ij} + \beta \Delta \sigma^e_{ij}) = 0 \qquad (3.2)$$

where the original stress σ_{ij} are such that :

$$f(\sigma_{ij}) < 0 \tag{3.3}$$

and β is the variable determined by solving the second order equation resulting from the use of Von Mises criterion.

3.1 *Generalised trapezoidal algorithm*:

The generalised trapezoidal algorithm is based on the following equations:

$$\mathbf{y}_{n+1} = \mathbf{y}_n + \Delta t\, \Phi_{n+} \tag{3.4}$$

$$\Phi_{n+\theta} = (1-\theta)\Phi(\mathbf{y}_n, t_n) + \theta\Phi(\mathbf{y}_{n+1}, t_{n+1}) \tag{3.5}$$

where, $\mathbf{y}_n$ is the known variable at time t_n, whereas $\mathbf{y}_{n+1}$ are the unknown variables at time $t_{n+1}=t_n+\Delta t$, Δt being the time step. The algorithmic parameter θ ranges from 0 to 1 so that :

- if $\theta=0$, the forward-Euler algorithm is obtained. This algorithm does not give stresses that satisfy the yield criterion (fully explicit scheme).
- if $\theta=1$ the backward-Euler algorithm is produced, which requires an iterative procedure at the Gauss-point level to solve the associated non-linear equations (fully implicit scheme).
- for other values of θ, a generalised trapezoidal algorithm is produced which is also an iterative type and become second order algorithm for $\theta=0.5$.

In this study, this algorithm has been used in conjunction with a self-adaptive step size control, where the time step size is regulated on the basis of a comparison between an estimated error at t_{n+1} and some desired accuracy . The truncated error is given by:

$$\delta = \frac{\Delta t_n^2}{2}(1-2\theta)\Phi(\mathbf{y}_n, t_n) + \frac{\Delta t_n^3}{6}(1-3\theta)\Phi(\mathbf{y}_n, t_n) \tag{3.6}$$

Therefore, if the error δ is smaller in magnitude than δ_0, the step size could be safely increased for the next step by using the following equation:

$$\Delta t_{n+1} = \min\left(k_1 \sqrt[3]{\frac{|\delta_0|}{\alpha|\delta|}}\Delta t_n, k_2 \Delta t_n\right) \tag{3.7}$$

with α, k_1 and k_2 being coefficients determined by numerical experiment.

However, despite the accomplished effort to solve accurately the constitutive equations (2.7-11) by adaptive step size control and a sufficient prescribed accuracy of the Newton-Raphson iterative technique, the algorithm produces stresses that lie outside the yield surface. To alleviate this disadvantage, the "coalescing" of the generalised trapezoidal and return mapping algorithms is proposed. In fact, the adaptive step size control has been removed because it is at the origin of the high CPU time and it is not sufficient to enforce the consistency condition. The computation is carried out by a fixed sub-step size, which is reduced by half whenever the maximal number of the Newton-Raphson technique is reached. Moreover, this suppression is replaced by the corrector process of the return mapping algorithm presented in section 3.3. The solution (does not necessary enforce the consistency condition) obtained by the generalised trapezoidal algorithm is considered like "plastic" prediction and then the stress is projected onto the yield surface by the relaxation process described in section 3.3. Thus, this procedure lead to a new kind of predictor-corrector algorithm giving a good results and satisfying a good compromise between performance and usefulness.

3.2 *Runge-Kutta algorithm*

The basic idea of the Runge-Kutta method is to find a solution over a time step by evaluating the right-hand side by many ways. The most often used one is the classical fourth- order Runge-Kutta formula [BUT 87] written as:

$$\mathbf{k}_1 = \Phi(\mathbf{y}_n, t_n) \tag{3.8a}$$

$$\mathbf{k}_2 = \Phi(\mathbf{y}_n + \frac{1}{2}\Delta t\mathbf{k}_1, t_n + \frac{1}{2}\Delta t) \tag{3.8b}$$

$$\mathbf{k}_3 = \Phi(\mathbf{y}_n + \frac{1}{2}\Delta t\mathbf{k}_2, t_n + \frac{1}{2}\Delta t) \tag{3.8c}$$

$$\mathbf{k}_4 = \Phi(\mathbf{y}_n + \Delta t\mathbf{k}_3, t_n + \Delta t) \tag{3.8d}$$

$$\mathbf{y}_{n+1} = \mathbf{y}_n + \frac{\Delta t}{6}(\mathbf{k}_1 + 2(\mathbf{k}_2 + \mathbf{k}_3) + \mathbf{k}_4) + o(\Delta t^5) \tag{3.9}$$

Another kind of the fourth-order Runge-Kutta formula is given by:

$$\mathbf{k}_1 = \Phi(\mathbf{y}_n, t_n) \tag{3.10a}$$

$$\mathbf{k}_2 = \Phi(\mathbf{y}_n + \frac{1}{3}\Delta t\mathbf{k}_1, t_n + \frac{1}{3}\Delta t) \tag{3.10b}$$

$$\mathbf{k}_3 = \Phi(\mathbf{y}_n - \frac{1}{3}\Delta t\mathbf{k}_1 + \Delta t\mathbf{k}_2, t_n + \frac{2}{3}\Delta t) \tag{3.10c}$$

$$\mathbf{k}_4 = \Phi(\mathbf{y}_n + \Delta t(\mathbf{k}_1 - \mathbf{k}_2 + \mathbf{k}_3), t_n + \Delta t) \tag{3.10d}$$

$$\mathbf{y}_{n+1} = \mathbf{y}_n + \frac{\Delta t}{8}(\mathbf{k}_1 + 3(\mathbf{k}_2 + \mathbf{k}_3) + \mathbf{k}_4) + \mathbf{o}(\Delta t^5) \tag{3.11}$$

The fourth-order Runge-Kutta method which is an explicit method is then a non-iterative, stable and accurate schema. However, it's an expensive one since it requires four evaluations of the right-hand side over each time step. This weakness is avoided when this integration method is combined with a self-adaptive scheme explained here below.

Adaptive step size control for Runge-Kutta scheme:

It is possible to associate with Runge-Kutta algorithm some adaptive control over its own progress. This allows numerical errors which are inevitably introduced into the solution. This latter can be controlled by automatic changing of the step size and can achieve some predetermined accuracy with a minimum computational effort. Implementation of adaptive step size control requires an estimation of its truncation error. To evaluate this error, two techniques can be adopted:

1°) The step doubling technique, where each step is taken twice, once as a full step of size $2\Delta t$, then independently, as two half steps each of size Δt. Let us consider $\mathbf{y}(t_n+2\Delta t)$ is the exact solution for an advance from t_n to $t_n+2\Delta t$ and $\mathbf{y}_1$ the numerical solution obtained from one step. The exact solution can be written as follows:

$$\mathbf{y}(t_n + 2\Delta t) = \mathbf{y}_1 + (2\Delta t)^5\varphi + \mathbf{o}(\Delta t^6) \tag{3.12}$$

and $\mathbf{y}_2$ obtained from two steps:

$$\mathbf{y}(t_n + 2\Delta t) = \mathbf{y}_2 + 2(\Delta t)^5\varphi + \mathbf{o}(\Delta t^6) \tag{3.13}$$

where φ is a vector of the magnitude $\frac{\mathbf{y}^{(5)}(t)}{5!}$. The difference between the two numerical solutions is a convenient indicator of truncation error,

$$\delta = \mathbf{y}_2 - \mathbf{y}_1 = 30\Delta t^5\varphi + \mathbf{o}(\Delta t^6) \tag{3.14}$$

This technique is expensive due to the several evaluations of the right-hand sides (11 evaluations).

2°) An alternative step size regulation technique as proposed in [TOU 93], based on the truncation error estimation without additional evaluation of the right-hand side. It consists of approximating this latter Φ in $[t_n,t_{n+1}]$ by a function $\overline{\Phi}$, which leads to approximate $\mathbf{y}$ by $\overline{\mathbf{y}}$, the integration of $\overline{\Phi}$.

Let $\mathbf{k}_1$, $\mathbf{k}_2$, $\mathbf{k}_3$, and $\mathbf{k}_4$ be the estimations of Φ given by (3.10). The approximate $\overline{\Phi}$ of Φ in $[t_n,t_{n+1}]$ is the Lagrange interpolate polynomial defined by:

$$\overline{\Phi}(t_n) = \mathbf{k}_1 \tag{3.15a}$$

$$\overline{\Phi}(t_n + \frac{\Delta t}{3}) = \frac{1}{12}(\mathbf{k}_1 + 9\mathbf{k}_2 + 3\mathbf{k}_3 - \mathbf{k}_4) \tag{3.15b}$$

$$\overline{\Phi}(t_n + \frac{2\Delta t}{3}) = \frac{1}{6}(-\mathbf{k}_1 + 3\mathbf{k}_2 + 3\mathbf{k}_3 + \mathbf{k}_4) \tag{3.15c}$$

$$\overline{\Phi}(t_n + \Delta t) = \frac{1}{4}(\mathbf{k}_1 - 3\mathbf{k}_2 + 3\mathbf{k}_3 + \mathbf{k}_4) \tag{3.15d}$$

By using the notation $x = \dfrac{t - t_n}{\Delta t}$ then $\overline{\Phi}$ can be written as,

$$\overline{\Phi}(t) = \overline{\mathbf{p}}(x) = \overline{\mathbf{a}}_2 x^2 + \overline{\mathbf{a}}_1 x + \overline{\mathbf{a}}_0 \tag{3.16}$$

where,
$$\overline{\mathbf{a}}_1 = -\frac{3}{2}(2\mathbf{k}_1 - 3\mathbf{k}_2 + \mathbf{k}_4) \tag{3.17a}$$

$$\overline{\mathbf{a}}_1 = -\frac{3}{2}(5(\mathbf{k}_1 - \mathbf{k}_2) - \mathbf{k}_3 + \mathbf{k}_4) \tag{3.17b}$$

(3.17c)

Let's suppose that:

$$\overline{\mathbf{q}}(x) = \mathbf{y}_n + \int_0^x \Delta t \overline{\mathbf{p}}(\xi) d\xi = \mathbf{y}_n + \int_{t_n}^t \overline{\Phi}(\tau) d\tau \tag{3.18}$$

One has :

$$\bar{\mathbf{q}}(x) = \mathbf{y}_n + \Delta t x(\frac{1}{3}\bar{\mathbf{a}}_2 x^2 + \frac{1}{2}\bar{\mathbf{a}}_1 x + \bar{\mathbf{a}}_0) \tag{3.19}$$

which leads for x = 1 to:

$$\bar{\mathbf{q}}(1) = \mathbf{y}_n + \frac{\Delta t}{8}(\mathbf{k}_1 + 3(\mathbf{k}_2 + \mathbf{k}_3) + \mathbf{k}_4) + \mathbf{o}(\Delta t^5) \tag{3.20}$$

This expression is the numerical solution of $\mathbf{y}(t)$ obtained by equation (3.11).

Consequently, an estimation of the approximate error ofΦ by $\overline{\Phi}$ is given by:

$$\begin{aligned} \bar{\mathbf{e}}(1) &= \bar{\mathbf{p}}(1) - \Phi(t_n + \Delta t, \bar{\mathbf{q}}(1)) \\ &= \bar{\mathbf{p}}(1) - \Phi(t_n + \Delta t, \mathbf{y}(t_n + \Delta t)) + \mathbf{o}(\Delta t^5) \end{aligned} \tag{3.21}$$

and the error on $\mathbf{y}$ is,

$$\delta = \frac{\Delta t \bar{\mathbf{e}}(1)}{4} \tag{3.22}$$

Now, the error is approximately known by two methods. The relationship between δ and the step size Δt is written as:

$$\Delta t_0 = S\Delta t\left|\frac{\delta_0}{\delta}\right|^{0.2} \tag{3.23}$$

where Δt_0 denotes the step that would give the desired accuracy δ_0 and S is a safety factor (equal to 0.9). This equation tells by how much the step size need to be decreased, when δ is larger than δ_0. Otherwise, the following relation is used to predict the size for the next step,

$$\Delta t_0 = S\Delta t\left|\frac{\delta_0}{\delta}\right|^{0.25} \tag{3.24}$$

Remark 1: This algorithm does not require any correction of stress to avoid drift from the yield surface including in the softening stage.
Remark 2: The second method of evaluating the truncated error is third order accurate, when the algorithm is a fourth order accurate.
Remark 3: The second technique of evaluating the error does not cost anything since no more evaluation of the right-hand side of the equations is required.

3.3 *Return mapping algorithm*:

Several return mapping algorithms have been used for the integration of the elastoplastic constitutive relations. For complex models, as in damage models, a return mapping algorithm with the operator splitting methodology proposed by [ORT 86] has been applied by [SIM 87] to their damage models. In accordance with the notion of the operator split, we consider an additive decomposition of equation (2.7-11) into the elastic part and plastic part.

Total	≡	Elastic part	+	Plastic part
$\dot{\varepsilon}_{ij}$ = given		$\dot{\varepsilon}_{ij}$ = given		$\dot{\varepsilon}_{ij} = 0$
$\dot{\sigma}_{ij} = L^{\sigma}_{ijkl}\dot{\varepsilon}_{kl}$		$\dot{\sigma}_{ij} = L^{\sigma e}_{ijkl}\dot{\varepsilon}_{kl}$		$\dot{\sigma}_{ij} = L^{\sigma p}_{ijkl}\dot{\varepsilon}_{kl}$
$\dot{\alpha}_{ij} = L^{\alpha}_{ijkl}\dot{\varepsilon}_{kl}$		$L^{\alpha}_{ijkl} = 0$		$\dot{\alpha}_{ij} = L^{\alpha p}_{ijkl}\dot{\varepsilon}_{kl}$
$\dot{r} = L^{r}_{ij}\dot{\varepsilon}_{ij}$		$L^{r}_{ij} = 0$		$\dot{r} = L^{rp}_{ij}\dot{\varepsilon}_{ij}$
$\dot{D} = L^{D}_{ij}\dot{\varepsilon}_{ij}$		$L^{D}_{ij} = 0$		$\dot{D} = L^{Dp}_{ij}\dot{\varepsilon}_{ij}$

Therefore, the return mapping algorithm may be viewed as an integration scheme with two steps: elastic predictor and plastic corrector.

Elastic predictor:

a)during the step n+1, the elastic trial stress is evaluated as:

$$\sigma^{(T)}_{ij_{n+1}} = \sigma_{ij_{n+1}} + L^{\sigma e}{}_{ijkl}\Delta\varepsilon_{kl_{n+1}} \tag{3.25}$$

$$\text{with,} \quad \varepsilon^{p(T)}_{ij_{n+1}} = \varepsilon^{p}_{ij_n}, \alpha^{(T)}_{ij_{n+1}} = \alpha_{ij_n}, r^{(T)}_{n+1} = r_n \text{ and } D^{(T)}_{n+1} = D_n \tag{3.26}$$

b) check for plastic yield,

if $f^{(T)}_{n+1} \le 0$ then

$$\varepsilon^{p}_{ij_n} = \varepsilon^{p(T)}_{ij_{n+1}}, \alpha_{ij_n} = \alpha^{(T)}_{ij_{n+1}}, r_n = r^{(T)}_{n+1} \text{ and } D^{(T)}_{n+1} = D_n \tag{3.27}$$

go to g)
if $f^{(T)}_{n+1} > 0$ then $i = 0$

Plastic corrector:

c) At this stage, the stresses are relaxed in a step-by-step process. For each iteration, the yield function f is linearized around the current values of the state variables obtaining:

$$f \approx f(\sigma^{(i)}_{ij_{n+1}}, q^{(i)}_{ij_{n+1}}) + \frac{\partial f}{\partial \sigma_{ij}}(\sigma^{(i)}_{ij_{n+1}}, q^{(i)}_{ij_{n+1}})(\sigma_{ij} - \sigma^{(i)}_{ij_{n+1}}) + \frac{\partial f}{\partial q_{ij}}(\sigma^{(i)}_{ij_{n+1}}, q^{(i)}_{ij_{n+1}})(q_{ij} - q^{(i)}_{ij_{n+1}}) \tag{3.28}$$

where, q_{ij} represents the internal state variables.

d) The plastic consistent parameter $\Delta\lambda$ is determined by requiring $f = 0$.

Then, the update stresses and internal state variables are:

$$\sigma^{(i+1)}_{ij_{n+1}} = \sigma^{(i)}_{ij_{n+1}} - \Delta\lambda[L^{\sigma e}_{ijkl}\frac{\partial F}{\partial \sigma_{kl}} - \frac{\partial F}{\partial Y}\frac{\sigma^{(t)}{}_{ij_{n+1}}}{1-D}] \tag{3.29}$$

$$\varepsilon^{(i+1)}_{ij_{n+1}} = \varepsilon^{(i)}_{ij_{n+1}} - \Delta\lambda\frac{\partial F}{\partial \sigma_{ij}} \quad ; \quad \alpha^{(i+1)}_{ij_{n+1}} = \alpha^{(i)}_{ij_{n+1}} + \Delta\lambda\frac{\partial F}{\partial X_{ij}} \tag{3.30}$$

$$r^{(i+1)}_{n+1} = r^{(i)}_{n+1} + \Delta\lambda\frac{\partial F}{\partial R} \quad ; \quad D^{(i+1)}_{n+1} = D^{(i)}_{n+1} + \Delta\lambda\frac{\partial F}{\partial Y} \tag{3.31}$$

e) if $\left|f^{(i+1)}_{n+1}\right| \le \varepsilon\left|f^{(T)}_{n+1}\right|$ then

$$\sigma_{ij_{n+1}} = \sigma^{(i+1)}_{ij_{n+1}} \; ; \; \varepsilon^{p}_{ij_{n+1}} = \varepsilon^{p(i+1)}_{ij_{n+1}} \; ; \; \alpha_{ij_{n+1}} = \alpha^{(i+1)}_{ij_{n+1}};$$
$$r_{n+1} = r^{(i+1)}_{n+1} \quad \text{and} \quad D_{n+1} = D^{(i+1)}_{n+1} \tag{3.32}$$

with, ε being the prescribed tolerance
otherwise, $i \leftarrow i+1$ go to c) .

g) Beginning the new sub-increment and go to a).

4. Numerical studies and applications:

The accuracy and robustness of the studied integration algorithms are evaluated in this section. These algorithms together with the Coupled Constitutive Equations (CCE) are implemented in the general purpose finite element code SIC (Système Intéractif de Conception). To study the numerical performance of these integration schemes, the simple case of Gauss point is treated and the results compared for various situations. The example of the cantilever beam studied by [TOU 93] is also treated using the CCE. In both cases the used material constants are those listed in the table I.

	Parameter	Value	Unit
- Isotropic elasticity	E	200000	MPa
	ν	0.3	-
- Yield stress	k	264	MPa
- Isotropic hardening	Q	1000	MPa
	b	16	-
- Kinematic hardening	C	10000	MPa
	a	20	-
- Isotopic damage	S	10	-
	s	1	-
	α	1	-

Table I. *Used materiel parameters*

The comparison has been performed for the following algorithms : Generalised trapezoidal algorithm with θ=0.5 (GTA), Runge-Kutta algorithm firstly with double step technique (RKA) and secondly with second technique of adaptive step size control (RKB), Return mapping algorithm (RMA), Forward-Euler algorithm (FEM) and Backward-Euler algorithm (BEM). Note that the numerical parameters used for the different schemes are ε=0.0001 RMA and GTA, δ_0=0.0001 for RKA and δ_0=0.00001 for RKB. For the Newton-Raphson scheme the maximum iterations number is 20 and the accuracy is 0.0001.

4.1 *At Gauss point level:*

The Gauss point is subjected to simple elongation (plane strain). The results of computation for the accuracy analysis are summarised in the figures 1 and 2. These figures show the variation of the equivalent stress versus the accumulated plastic

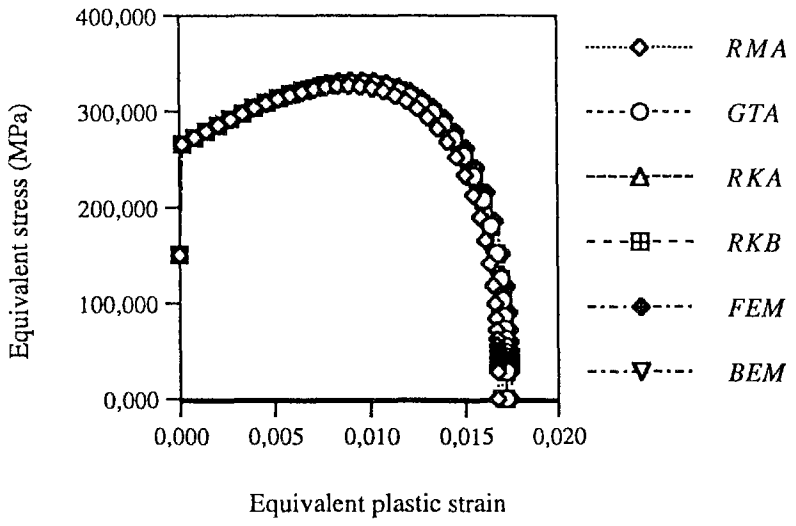

Figure 1. *The equivalent stress-strain σ–ε in small deformation (SS), dt = 0.001*

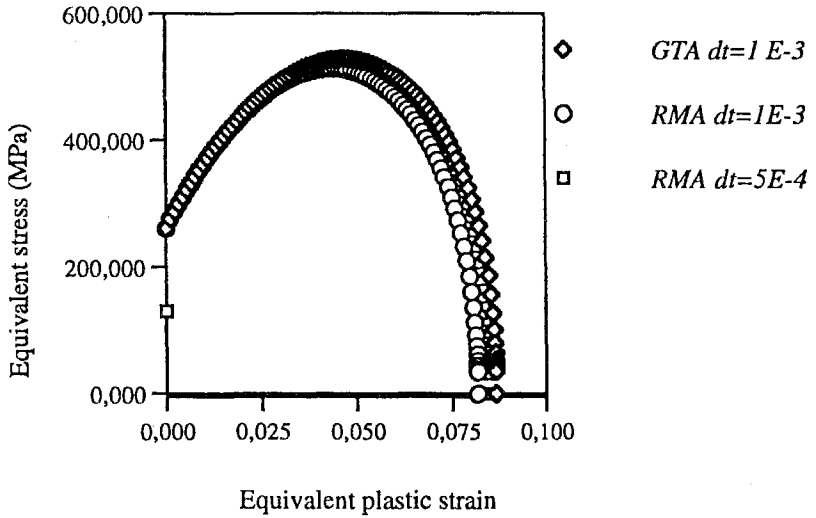

Figure 2. *The equivalent stress-strain σ–ε in large deformation (LS)*

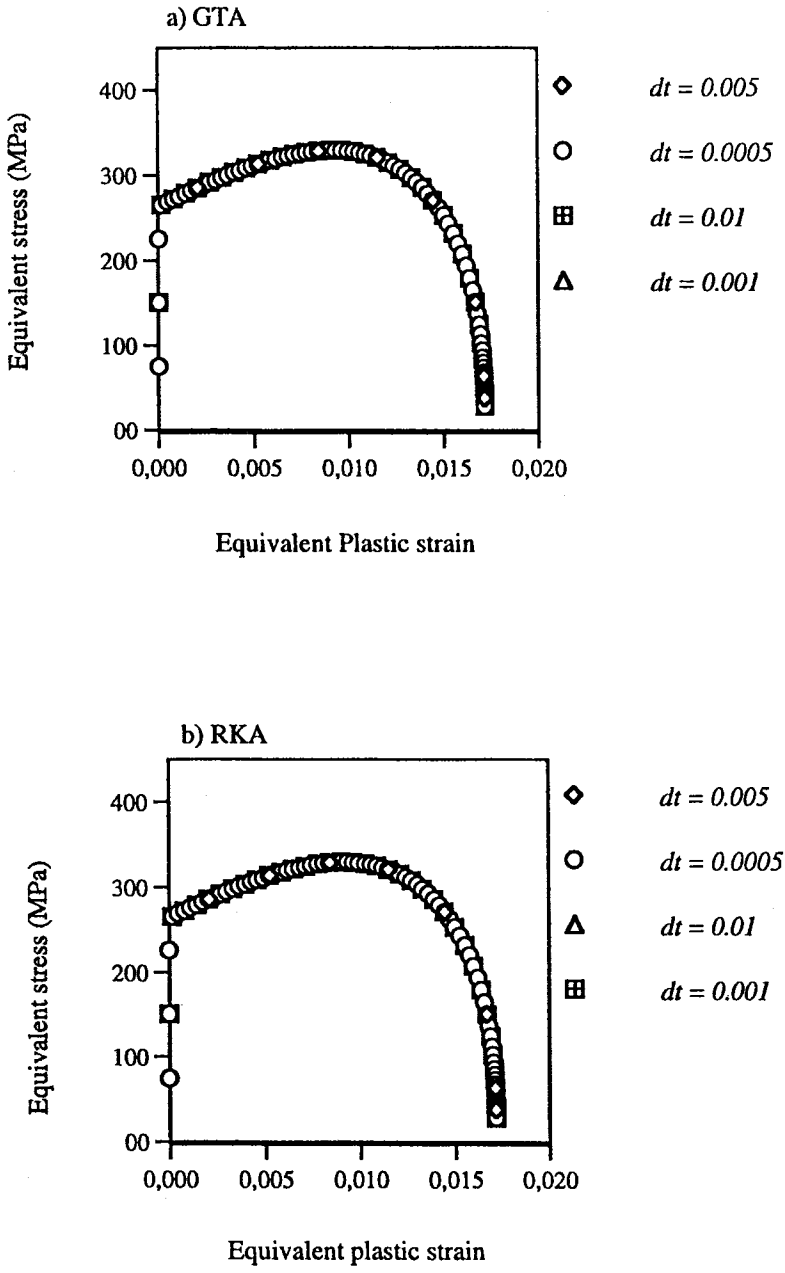

Figure 3. *Stability of the integration procedures*

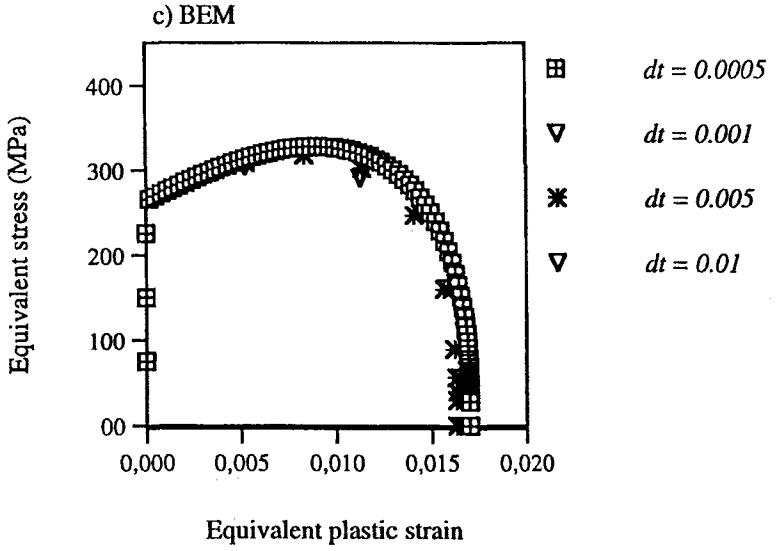

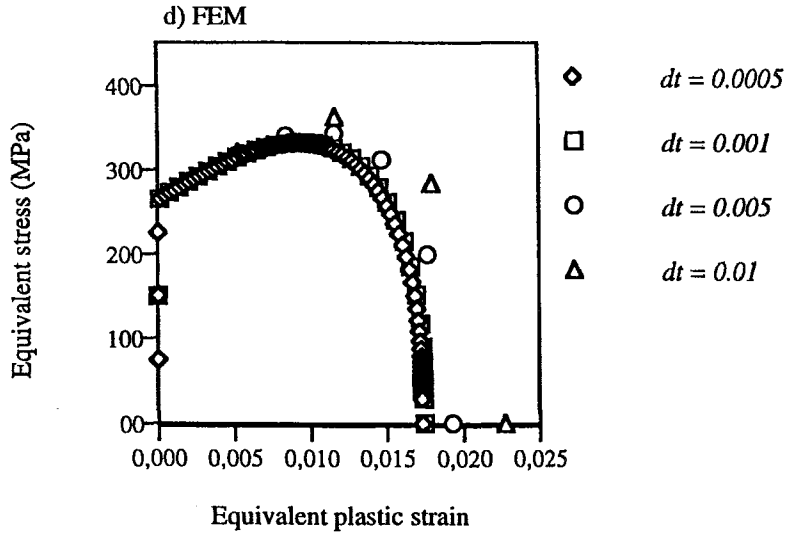

Figure 3. *Stability of the integration procedures*

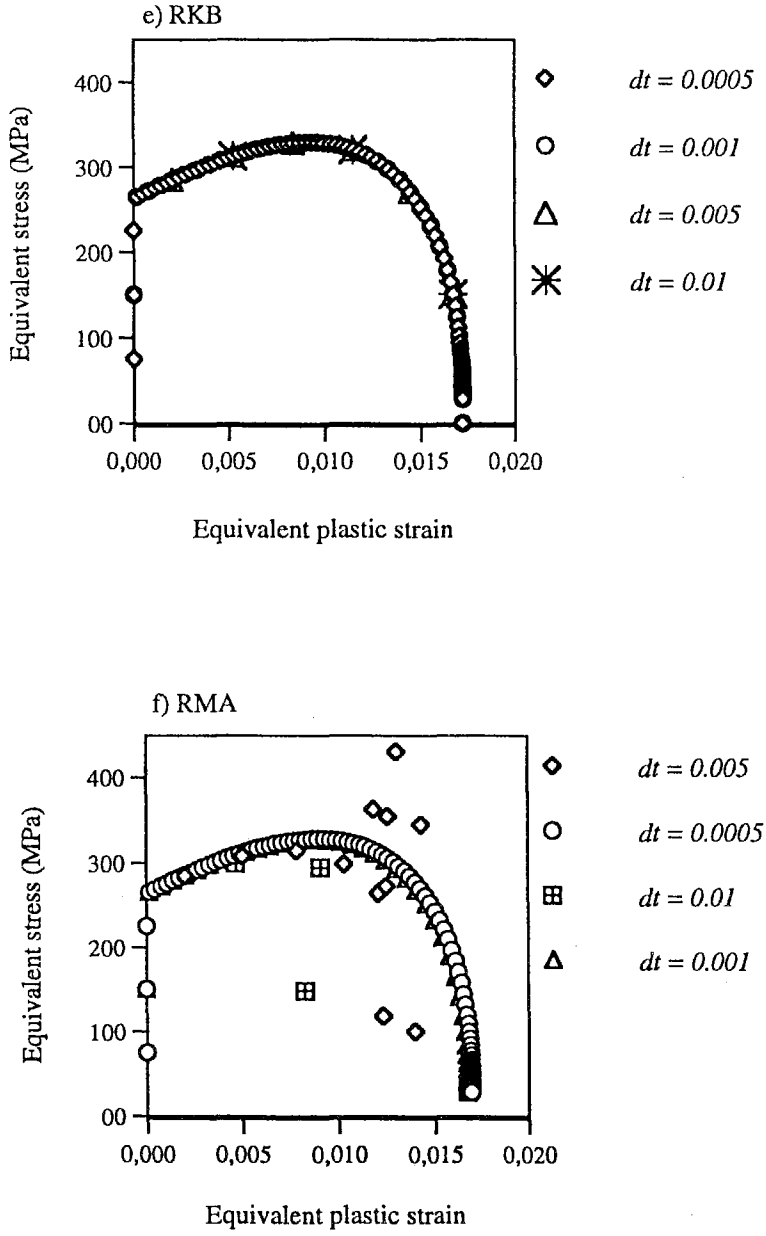

Figure 3. *Stability of the integration procedures*

strain, the curve corresponding to the smallest increments is taken as the 'reference' numerical solution. These curves show clearly the softening stage induced by the damage effect i.e. the stress reaches a maximum value (σ_{max} = 350.0 MPa for the small strain (SS) case and σ_{max} = 550.0 Mpa for the large strain (LS) case) and decrease going to zero. The equivalent plastic strain at fracture is P_f=1.7 % in the SS case and P_f=9 % in the LS case. Figure 1 shows that the numerical solutions obtained by all the algorithms are almost identical. However, the solution of the return mapping algorithm deviates slightly from the others. This difference is more important in LS case, where it decreases when the time step size decreases (see figure 2).

The figures (3a to 3f) are plotted to show the stability and the accuracy of the procedures as the time step size is increased. It appears that, before the softening stage, the numerical solution is stable for all algorithms as it is observed in the case of classical elastoplastic model. After the softening stage where the effect of damage is more important, the RKA, RKB and GTA algorithms present a stability in this stage. However, the other algorithms become no accurate. In fact, the RMA scheme gives a wrong solution and the FEM and BEM schemes produce a solution changing when increasing the step size. These differences can be explained by the high non linearity of the constitutive equations when the damage is taken into account. Therefore, the resolution requires a small time step size to have a stable numerical procedure. Whereas, the stability of some algorithms is due to the high order accuracy of the Runge Kutta algorithms in conjunction with adaptive step size control and for the iterative algorithms where the accuracy is always assured throughout iterations.

	CPU time					
dt	RMA	GTA	RKA	RKB	FEM	BEM
0.0005	1.6	3.8	2.3	1.9	2.6	4.0
0.0010	1.2	3.4	2.1	1.7	2.1	3.7
0.0050	-	1.1	0.8	0.7	0.1	0.2
0.0100	-	0.2	0.6	0.6	0.1	0.2

Table II. *Comparison of CPU time (Dec Station 5000/200).*

Moreover, comparison of CPU time indicates that the amounts of CPU times are quite different. Table II shows that, for small step size, the RMA scheme is more efficient computationally than the RKB scheme which is faster than the others and it

consumes 1.2 more CPU time than RMA scheme. However, as the size of time steps increases, this latter is not stable and the efficiency of RKA, RKB becomes comparable. This result is justified by the fact that although the second technique of adaptive control size shown in previous section does not cost anything, the error evaluation is less accurate. Thus, this leads to the small sub-step size and then many more sub-steps for each load step (see figures 4 and 5), in comparison to the step doubling technique where the error estimation is more accurate and the control of the step size is more efficient. Consequently, this costly latter algorithm scheme becomes computationally comparable to the previous one when the step size increases. The table II shows also that the GTA is more efficient for large step size, it consumes 3 times less of CPU times than RKA and RKB.

Another aspect can be demonstrated in this algorithm analysis for checking the plastic consistency condition, i.e., the states of stress computed from the algorithms remain always within the elastic domain. Figure 6 shows the evolution of the yield function during the numerical integration. All the algorithms enforce the consistency condition as shown in figure 6. The iterative procedures satisfy normally the consistency condition because of the stress correction. While, in the case of the explicit Runge-Kutta algorithm, this satisfaction is realised without any need to correction process. In addition, the figures 7 and 8 show for this latter algorithm that the consistency condition is more enforced when the size of the time step or the prescribed accuracy are increased. The same comment can be made for the RKA algorithm.

4.2 *At structural level:*

To analyse the performance of the studied algorithms the well known example of a straight cantilever beam under a prescribed displacement applied at its free end is considered [BRA 86]. The geometry and mesh involving 8 nodes quadrilateral elements are shown in figure 9. The simulation are conducted with finite element code SIC, where, the calculations are performed in finite elastoplasticity fully coupled with damage under the assumption of plane stress and Jaumann objective derivative. The material properties are the same given in table I. Note that in the classical elastoplasticity without damage the obtained results match closely with those given in [TOU 93]

The cantilever beam is bent until the displaced point cover a distance equal to the width of the beam. The finite element analysis of this case with an efficient CPU time require a computation with a large increment of time . It's worth noting that the CPU time for this example (Dec Station 5000/200) was 729.39 s for RKB, 840.82 s for GTA and 941.62 s for RKA.

The table III summarises some typical results for the coupled case obtained inside the elements number 4, 5, and 48 shown in the figure 9. The values obtained with smallest increments ($\Delta t = 0.0005$) are taken as the reference numerical solution.

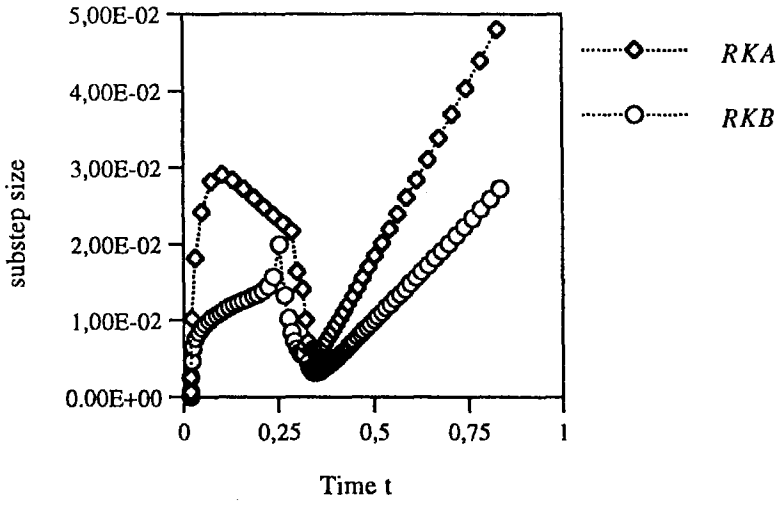

Figure 4. *Evolution of the substep size through the integration.*

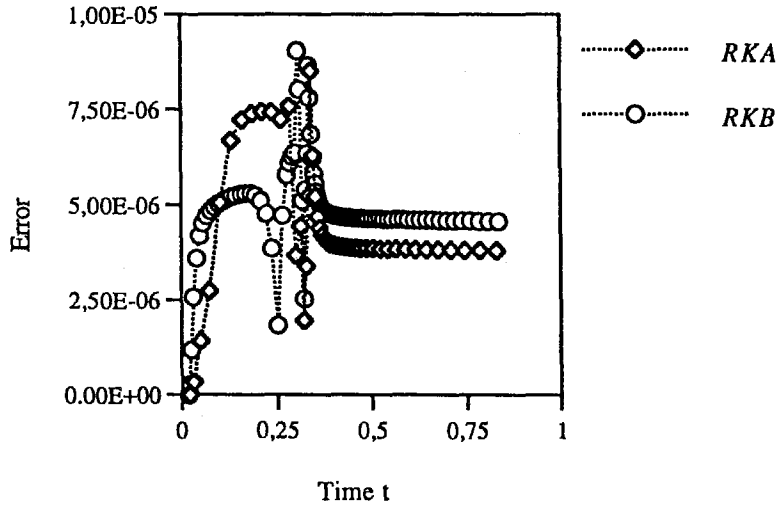

Figure 5. *Evolution of the error through the integration*

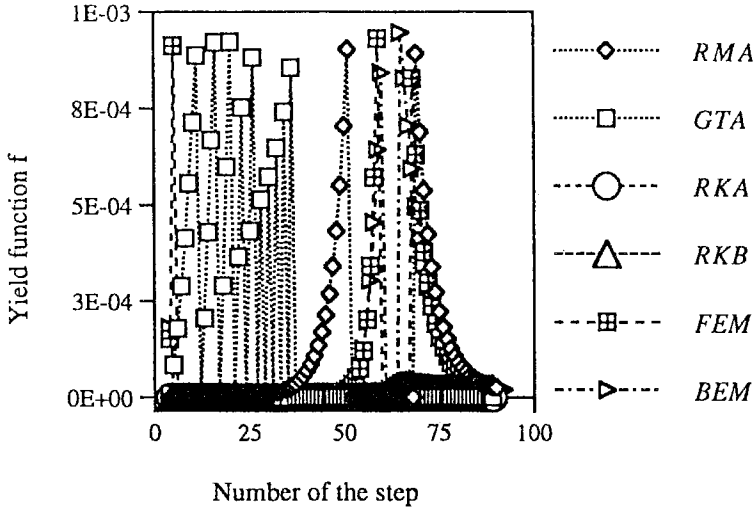

Figure 6. *Evolution of the yield function*

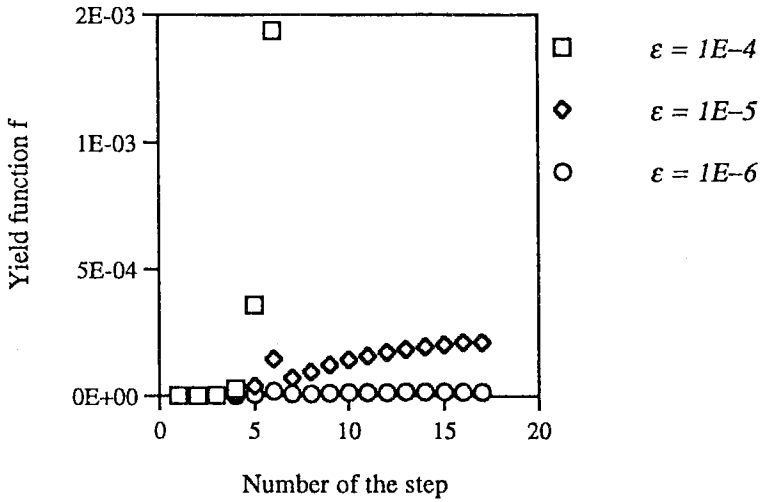

Figure 7. *Effect of the prescribed accuracy on the consistency condition (RKB)*

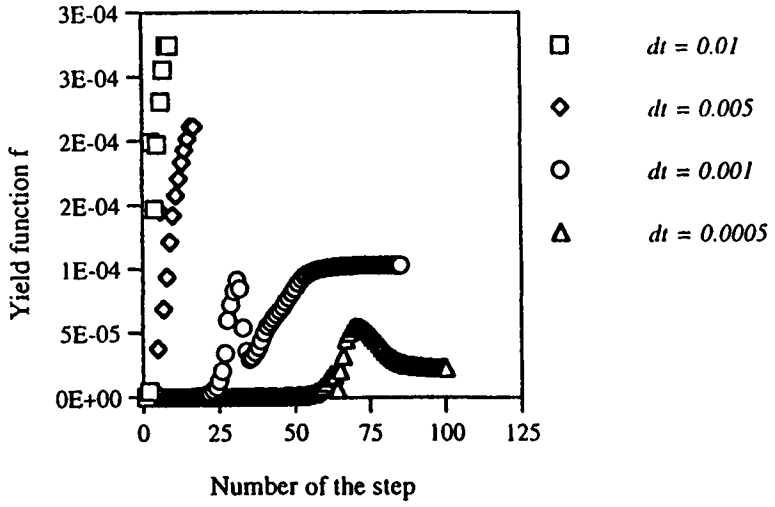

Figure 8. *Effect of step size on the consistency condition (RKB).*

From these results we can observe that for the element 4, where the reference value of the damage is 0.45, the GTA, RKA and RKB schemes gives the closest solutions while the RMA schemes gives a very different solution (i.e. fully fracture of the element). Hence this algorithms needs a smallest value of the time step to get a better solution.

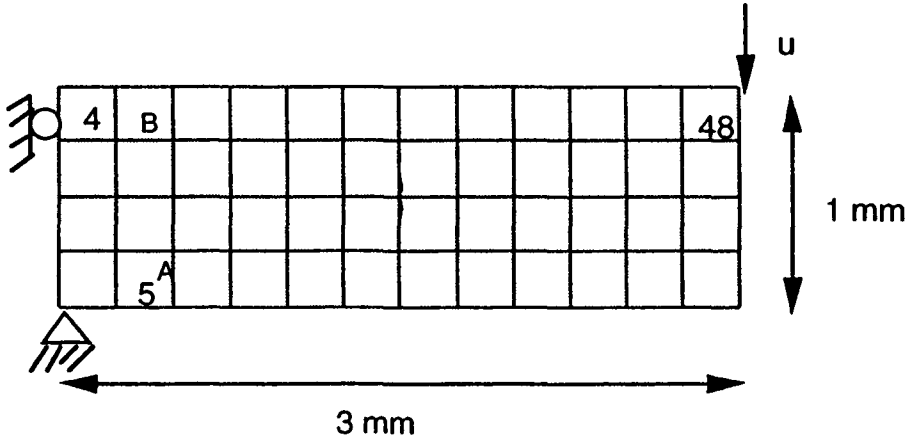

Figure 9. *The Geometry and the mesh of the cantilever beam*

For the element 5 the same conclusion can be made where we can clearly see that the better solutions are given by the Runge-Kutta algorithms. Note that for the fully damaged element the stress is zero (i.e. when the value of the damage at each Gauss-point reaches 0.99), the Moduli E, C and Q are explicitly put equal to zero as indicated in the constitutive equations. The figure 10 shows the iso-damage inside the cantilever beam. One can notice that the damage initiates inside the element 5 and propagates in the direction normal to the axis of the beam.

Figure 11 shows the global response of the beam throughout a variation of the global effort F versus the displacement U. It can easily be noticed that as expected, F increases as U increases as long as the local damage D is negligible. As the damage becomes significant, the variation of the related variables F and U is quite different.

Element	Algorithms	σ_x	σ_y	σ_{xy}	p	D
4	Reference	697.72	57.73	60.48	0.2825	0.4509
	RMA	0.00	0.00	0.00	0.3142	1.0000
	GTA	700.61	56.59	59.18	0.2811	0.4464
	RKA	696.14	54.39	59.76	0.2819	0.4491
	RKB	696.14	54.39	59.76	0.2819	0.4491
	FEM	704.46	42.20	53.48	0.2752	0.4252
	BEM	668.28	51.49	68.73	0.2877	0.4755
5	Reference	0.00	0.00	0.00	0.3590	0.9964
	RMA	0.00	0.00	0.00	0.3307	1.0000
	GTA	0.00	0.00	0.00	0.3589	1.0000
	RKA	0.00	0.00	0.00	0.3588	0.9968
	RKB	0.00	0.00	0.00	0.3588	0.9968
	FEM	0.00	0.00	0.00	0.3628	0.9978
	BEM	0.00	0.00	0.00	0.3509	1.0000
48	Reference	-341.17	-120.46	89.87	0.0010	0.2454E-4
	RMA	-306.17	-128.76	91.52	0.0010	0.2394E-4
	GTA	-342.40	-121.05	90.09	0.0010	0.2458E-4
	RKA	-342.25	-121.05	90.08	0.0010	0.2458E-4
	RKB	-342.25	-121.05	90.08	0.0010	0.2458E-4
	FEM	-345.58	-120.11	89.45	0.0010	0.2452E-4
	BEM	-337.45	-121.42	90.15	0.0010	0.2459E-4

Table III. *Numerical results for some integration points* ($\Delta t = 0.01$)

In fact, the presence of the damage tends to reduce the value of the global effort when the displacement reaches a critical value. In this case of loading, the critical value of U is of about 0.75 mm corresponding to the maximum force F_{max} = 70.0 N. This traduces the weakness of the structure which is induced by the damage.

Figures 12 and 13 show the local responses of the points A and B located inside two elements as shown in the figure 10. These figures present the typical variation of the local stress versus local accumulated plastic strain for the first damaged Gauss point (figure 12); and for the neighbouring point where the elastic unloading takes place after some value of the local damage (figure 13). This unloading in the point B is due to the fully damaged state of the point A.

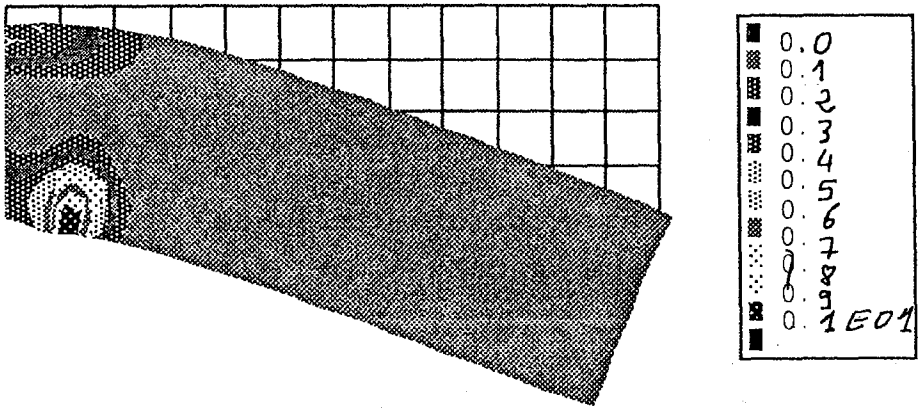

Figure 10. *Damage distribution inside the deformed cantilever beam*

5. Conclusion

The present work is an extension of the work by Touzot and Dabounou [TOU 93] to the fully coupled constitutive equations characterised by induced softening behaviour. For the non coupled constitutive equations, the results obtained in this reference are recovered. However for the case of fully coupled constitutive equations, the following conclusion can be made:

* The Runge-Kutta schemes (RKA and RKB) together with the GTA schemes are stable and accurate.

* The BEM and FEM schemes are enough accurate but need a very large CPU time.

* The RMA scheme is the less efficient one.

Hence, on the light of the examples studied herein, the Runge-Kutta schemes seems to be very interesting in regards to the implementation facilities (explicit schemes). The implicit scheme GTA has a very interesting numerical properties but its numerical implementation is less simple.

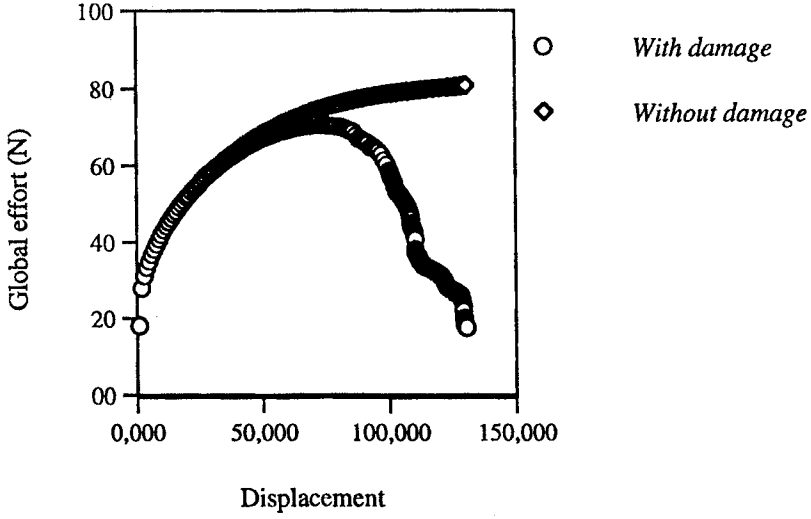

Figure 11. *Global effort vs dispalcement*

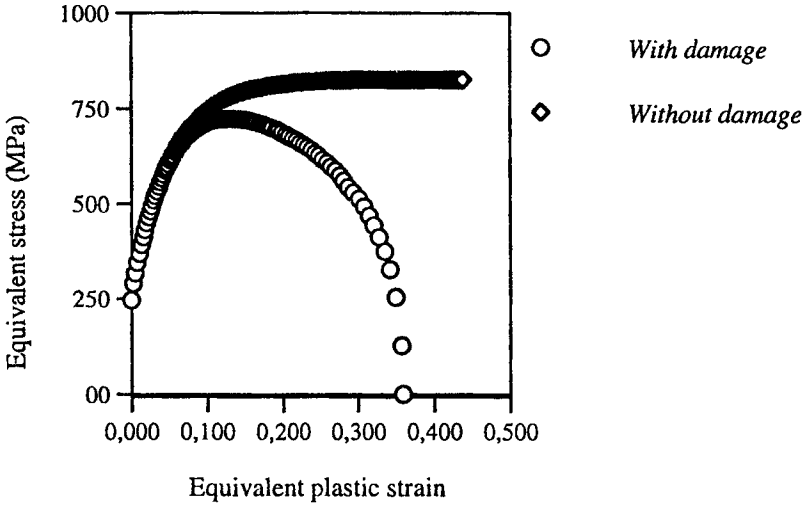

Figure 12. *Local response at point A*

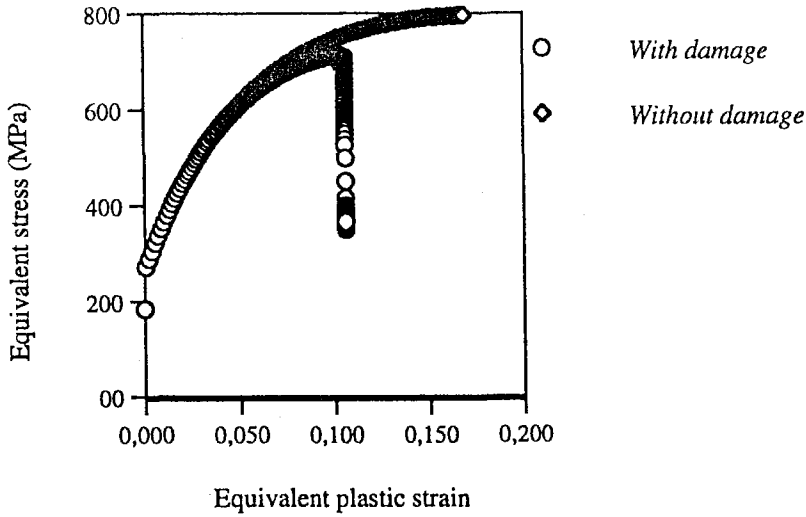

Figure 13. *Local response at point B*

References

[BEN 89] BENALLAL, A., «Thermo-viscoplasticité et endommagement des structures», Thèse de Doctorat Es Sciences, Paris VI, 1989.

[BEN 94] BEN HATIRA F., FORSTER CH., SAANOUNI K., «Prediction of Anelastic Flow Localization in Finite Elastoplasticity with Damage», Revue Européenne des éléments finis, vol. 3,p. 27-56. 1994.

[BEN 91] BEN HATIRA F., FORSTER CH., SAANOUNI K., «Modélisation Mécanique et Numérique des structures anélastiques endommageables», Rapport DRET, n° 90-111 UTC, 1991.

[BRA 86] BRAUDEL J. H., «Modélisation numérique des grandes déformations élastoplastiques d'un solide isotrope par la méthode des éléments finis.», Thèse de Doctorat d'Etat, Université Claude Bernard Lyon 1, 1986

[BUT 87] BUTCHER,J.C, «The numerical Analysis of Ordinary Differential Equations, Runge Kutta and general linear methods», John Willey & Sons.1987.

[CRI 91] CRISFIELD M.A, «Non-linear Finite Element Analysis of solids and structures», Volume 1. Willey. 1991.

[DOG 89] DOGUI A., «Plasticité anisotrope en grandes déformations», Thèse de Doctorat d'Etat, Université Lyon 1, 1989.

[ELM 89] El MOUATASSIM M., «Modélisation en grandes transformations des solides massifs par éléments finis», Thèse de doctorat, Div. Modèles Numériques en Mécanique, Université de Technologie de Compiègne, Novembre 1989.

[FOR 95] FORSTER, C., «Contribution à la rupture ductile des structures elastoplastiques», Thèse de Doctorat de l'Université de Technologie de Compiègne, 1995.

[GEL 85] GELIN J.C, «Modèles numériques et expérimentaux en grandes déformations plastiques et endommagement de rupture ductile», Thèse d'état, Université P. et M. Curie, Paris VI, 1985.

[GEL 92] GELIN J.C and DENESCU A., «Constitutive model and computational strategies for finite elasto-plasticity with isotropic or anistropic ductile damage», Computational Plasticity - Fundamentals and applications. Proceedings of the third International Conference , Part II 1413, Barcelona , Spain, 1992.

[GOL 89] GOLINVAL J.C , «Calcul par éléments finis des structures élasto-viscoplastiques soumises à des chargements cycliques à haute température», Thèse de Doctorat, Université de Liège, Belgique, 1989.

[LAD 80] LADEVEZE P., «Sur la théorie de la plasticité en grandes déformations», Rapport interne, ENS-LMT, n°9, 1980.

[LEM 85] LEMAITRE J., CHABOCHE J.L, «Mécanique des Matériaux solides», Dunod, Paris, 1985.

[ORT 86] ORTIZ M. and SIMO J.C., "«An Analysis of a New Class of Integration Algorithms for Elastoplastic Constitutive Relations», int. j. num. methods. eng., vol. 23, 353-366. 1986.

[ORT 85] ORTIZ M. and POPOV E.P., «Accuracy and Stability of Integration Algorithms for Elastoplastic Constitutive Relations», int. j. num. Meth. eng., vol. 21, 1561-1576. 1985.

[PRE 86] PRESS W.H, FLANNERY B.P., TEUKOLSKY S.A., VETERRELING W.T., «Numerical Recipes; The Art of Scientific Computing ». Cambridge University Press. 1986.

[NGU 72] NGUYEN Q.S , ZARKA J., «Quelques méthodes de résolution numérique en plasticité calssique et en viscoplasticité», Plastcité et Viscoplasticité, L.M.S, Ecole Polytechnique , 1972.

[SIM 84] SIMO J.C., TAYLOR R.L., «Consistent tangent Operators for rate-independent Elastoplasticity». Comp. Meth. Appl. Mech. Eng., 48, 101-118. 1984.

[SIM 86] SIMO J.C., TAYLOR R.L., «A return Mapping Algorithm for plane stress Elastoplasticity»., inter. j. num. methods. eng., 22, 649-670. 1986.

[SIM 87] SIMO J.C., JU J.W., «Stress and Strain Based continuum Damage Models. Part I: Formulation. Part II: Computational Aspects» Int. J. Solids Struc., 23(7):821-864,1987.

[SAA 94] SAANOUNI K., BENHATIRA F., FORSTER Ch., «On the Anelastic flow with damage», inter. j. damage. Mech, vol. 3, 140-169. 1994.

[TOU 93] TOUZOT G., DABOUNOU J., «Intégration numérique de lois de comportement élastoplastique», Revue Européenne des éléments finis, vol. 2, p. 465-492. 1993.

[WIL 89] WILLIAM K.J., «Recent Issues in Computational Plasticity», Proceedings of the Second International Conference held in Barcelona, Spain, September, 1989.

Acknowledgments

The authors gratefully acknowledge the financial support of the Conseil Régional de Picardie in the framework of the Pôle Modélisation.

Article soumis le 10 avril 1996.
Version révisée le 20 septembre 1996.